Acta Crystallographica Section B
Structural Science
ISSN 0108-7681

Structure of $Nd_{10}W_{22}O_{81}$ from high-resolution electron microscopy and X-ray powder diffraction

Carl Grenthe,[a]* Antonietta Guagliardi,[b] Margareta Sundberg[a] and Per-Erik Werner[a]

[a]Department of Inorganic and Structural Chemistry, Arrhenius Laboratory, Stockholm University, S-106 91, Stockholm, Sweden, and [b]C.N.R.-IRMEC c/o Dipartemento Geomineralogico, Universitario di Bari, Campus Universitario, Via Orabona 4, 70125 Bari, Italy

Correspondence e-mail: kalle@inorg.su.se

Received 1 June 2000
Accepted 26 September 2000

The crystal structure of $Nd_{10}W_{22}O_{81}$, neodymium tungstate, has been determined using a combination of high-resolution transmission electron microscopy and X-ray powder diffraction methods. The unit-cell dimensions determined from X-ray data are $a = 3.8613$ (1), $b = 35.9431$ (1), $c = 21.8900$ (1) Å, $V = 3038.05$ Å^3, $Z = 2$, space group *Pbcm*. The structure is built up of pentagonal columns (PCs) connected to ReO_3-type fragments consisting of three octahedra, thus forming W_9O_{32} units. These units form 'pillars' along **a**. These 'pillars' are joined by pairs of tilted octahedra (W_2O_{11} groups) to form corrugated layers perpendicular to **b**. The Nd atoms are located in the space between these layers and form the only link between them. Interstitial O atoms are located between two of the Nd atoms. The formula $Nd_{10}W_{22}O_{81}$ can thus be alternatively given as $Nd_5W_{11}O_{39+x}$ ($x \simeq 1.5$), where x represents the interstitial O atoms. $Nd_{10}W_{22}O_{81}$ is a new type of PC structure.

1. Introduction

Phase analysis studies of the system Ce_2O_3–WO_3 have revealed six stable phases with the mole ratios Ce_2O_3:WO_3 of 3:1, 3:2, 1:1, 1:3 and 2:9 (Yoshimura *et al.*, 1973, 1976). The 1:3 phase, which corresponds to the known cerium tungstate $Ce_2(WO_4)_3$, was reported to decompose into the 2:9 and CeO_2 phases at temperatures below 1073 K in air and below 1123 K in an oxygen atmosphere. The stoichiometric composition of the 2:9 product was reported to be between 17.5 and 19 mol% Ce_2O_3. It was also observed that this compound did not have solid solution regions and that it melted congruently at 1300 K. Furthermore, it was reported as a stable phase in the systems RE_2O_3–WO_3 with RE = La, Pr and Nd, but not in the systems Sm_2O_3–WO_3 or Y_2O_3–WO_3.

Further preparation and X-ray diffraction studies of the $2RE_2O_3{\cdot}9WO_3$ products with RE = La–Nd have resulted in the new stoichiometric formula $RE_{10}W_{22}O_{81}$. The unit-cell dimensions and the space group *Pbcn* have been given, but no structure model has been presented so far (Yoshimura *et al.*, 1975). Recently, Shimazaki *et al.* (1999) have studied double oxides in the system Pr_2O_3–WO_3. They prepared the 1:4.4 oxide ($Pr_{10}W_{22}O_{81}$) and determined the unit-cell dimensions from the X-ray diffraction data.

During a high-resolution transmission electron microscopy (HRTEM) study, undertaken to clarify the microstructure of RE_xWO_3 bronzes prepared at high temperature and ambient pressure conditions, we observed some crystals of a new structure type. The electron diffraction (ED) data and the microanalysis results indicated that these crystals could be the $RE_{10}W_{22}O_{81}$ phase, previously described by Yoshimura *et al.*

(1975). Samples of composition $RE_{10}W_{22}O_{81}$ were later synthesized for further structure analysis studies. In this study we will report the synthesis of the neodymium compound and the structural investigations of this compound by using a combination of X-ray powder diffraction and electron microscopy methods. A new type of crystal structure will be presented and discussed.

2. Experimental

2.1. Preparation

Samples of composition $5Nd_2O_3{\cdot}22WO_3$ were synthesized by a solid-state reaction between Nd_2O_3 and WO_3 (99.9 and 99.998%, respectively; Johnson & Matthey). The initial ingredients were mixed in an *n*-hexane slurry and then ground in an agate mortar and finally heated in an Al_2O_3 crucible at 1225 K in air for 36 h. The resulting powders were subsequently remixed and heated again at 1250 K for another 24 h. The products had a faint purple colour and looked fairly homogenous and microcrystalline under the optical microscope.

2.2. X-ray diffraction

An X-ray powder diffraction photograph was taken in a subtraction geometry Guinier–Hägg focusing camera with strictly monochromated Cu $K\alpha_1$ radiation (λ = 1.540598 Å). Reference material 640*b* (silicon) from the National Bureau of Standards was added as an internal 2θ standard. The photograph was measured with an automatic microdensitometer (Johansson *et al.*, 1980). The positions of the silicon lines were used to correct for sample displacement, zero-point error and film shrinkage. The X-ray powder pattern was indexed and the unit-cell parameters refined using the program *PIRUM* (Werner, 1969).

X-ray diffraction data for structure determination and refinement were collected on a Stoe Stadi/P powder diffractometer with a rotating sample in the symmetric transmission mode. A symmetric focusing germanium monochromator (focal distance = 440 mm) was used to give pure Cu $K\alpha_1$ radiation. The diffraction data were collected with a small linear position-sensitive detector (PSD) covering 6.4° in 2θ. The PSD was moved in steps of 0.2°, 400 s per step, thus giving an average of 32 measurements at each 2θ position. The 2θ range measured was $8 < 2\theta < 95°$. The peak shapes could be described by a symmetric pseudo-Voigt function.[1]

2.3. Electron microscopy

The electron-microscopy specimens were prepared in the following way. A small amount of the sample was crushed in an agate mortar and suspended in *n*-butanol, and finally a drop of the suspension was placed on a perforated carbon film supported on a copper grid. The grids were then examined in a JEOL 2000FXII transmission electron microscope (TEM), equipped with a LINK AN10000 EDS microanalysis system. Many crystals were studied using selected-area electron diffraction in combination with energy-dispersive X-ray spectroscopy (EDS analysis) on the same crystal fragment. The microanalysis results were based on the W(*L*) and the Nd(*L*) peaks in the EDS spectra.

The HRTEM images were taken in a JEOL 3010 TEM (URP 31 pole-piece, double-tilt, side-entry stage and with a tilt of ±10–20°) at 300 kV. The radius of the objective aperture used corresponded to 0.68 $Å^{-1}$ in reciprocal space. Crystallographic image processing (CIP) with the computer program system *CRISP* (Hovmöller, 1992) was applied to some HRTEM images. Theoretical HRTEM images were calculated using a locally modified version of the *SHRLI* set of programs (O'Keefe *et al.*, 1978).

Table 1
Experimental details.

	This study	Yoshimura *et al.* (1975)
a (Å)	3.8613 (1)	3.877 (1)
b (Å)	35.9431 (1)	35.971 (9)
c (Å)	21.8900 (1)	21.846 (6)
V ($Å^3$)	3038.05	3046.64
D_{calc} (g cm^{-3})	7.373	7.394
Space group	*Pbcm*(57)	*Pbcn*(60)
Z	2	2
Formula weight	6783.1	6783.1
R_F	0.127	
R_P	0.062	
R_{wp}	0.084	

3. Results

The unit-cell parameters given in Table 1 are very close to those reported for $Nd_{10}W_{22}O_{81}$ by Yoshimura *et al.* (1975). The indexed diffraction pattern up to $2\theta = 52°$ is presented in Table 2. A few lines from WO_3 have been subtracted from the diffraction pattern. Reflections with indices (*0kl*) were observed only for $k = 2n$ and (*h0l*) only for $l = 2n$, which is characteristic of space groups *Pbcm*, *Pbcn* and $Pbc2_1$. As can be seen from Table 2, however, space group *Pbcn* proposed by Yoshimura *et al.* (1975) should be excluded because of the presence of two (*hk*0) reflections with $h + k = 2n + 1$ in the high-angle region. Below $2\theta = 45°$, however, all systematic absence conditions are in agreement with space group *Pbcn* and as the presence of impurities could not be excluded, this space group was assumed in the preliminary electron microscopy study.

3.1. Electron microscopy

The electron diffraction pattern inserted in the corresponding HRTEM image in Fig. 1(*a*) is taken from a thin crystal fragment aligned with the 3.8 Å axis parallel to the electron beam. The pattern shows systematic absences for 0*kl* reflections when $k = 2n + 1$. This extinction condition fits with the space groups given above. Fig. 1(*b*) illustrates that the

[1] Supplementary data for this paper are available from the IUCr electronic archives (Reference: OS0061). Services for accessing these data are described at the back of the journal.

Table 2
X-ray powder diffraction data for $Nd_{10}W_{22}O_{81}$.

h	k	l	$2\theta_{obs}$ (°)	$2\theta_{calc}$ (°)	d_{obs} (Å)	I_{obs}
0	6	0	14.766	14.758	5.99	3.82
0	2	4	16.933	16.938	5.23	9.05
0	6	3	19.148	19.149	4.631	4.68
0	8	1	20.160	20.138	4.401	3.63
0	6	4	21.989	21.983	4.039	4.43
0	4	5	22.596	22.589	3.931	5.02
1	1	0	23.093	23.077	3.848	13.98
1	1	1	23.413	23.437	3.796	48.25
1	0	2	24.352	24.361	3.652	20.04
1	3	1	24.460	24.472	3.636	23.43
0	10	0	24.723	24.720	3.598	49.82
0	6	5	25.187	25.183	3.533	8.19
0	8	4	25.627	25.626	3.473	97.84
1	1	3	26.135	26.151	3.406	14.19
0	4	6	26.375	26.366	3.376	26.11
1	3	3	27.069	27.088	3.291	50.52
0	10	3	27.632	27.623	3.225	21.86
1	1	4	28.324	28.326	3.148	100.00
0	6	6	28.644	28.640	3.114	18.84
1	7	0	28.839	28.838	3.093	12.44
0	2	7	28.992	28.990	3.077	45.57
1	3	4	29.178	29.199	3.058	5.23
1	6	3	30.064	30.053	2.970	10.65
1	7	3	31.392	31.389	2.847	28.02
1	9	0	32.150	32.149	2.782	18.60
0	0	8	32.746	32.739	2.733	18.10
1	7	4	33.244	33.237	2.693	34.39
1	2	6	34.140	34.119	2.624	8.13
0	8	7	34.961	34.943	2.564	16.29
1	9	4	36.174	36.201	2.4811	23.86
1	8	5	36.865	36.852	2.4362	2.59
1	1	7	37.029	37.027	2.4258	6.22
1	3	7	37.703	37.719	2.3840	1.88
1	7	6	38.146	38.128	2.3573	3.57
1	5	7	39.080	39.072	2.3031	18.84
0	6	9	40.014	40.008	2.2514	8.19
1	3	8	41.093	41.080	2.1948	2.19
0	10	8	41.430	41.453	2.1777	10.07
1	9	7	43.539	43.528	2.0770	3.94
1	9	8	46.524	46.543	1.9504	29.13
2	3	0	47.517	47.520	1.9120	2.62
2	4	1	48.229	48.208	1.8854	7.57
2	5	2	49.395	49.403	1.8436	2.99
2	0	4	49.905	49.919	1.8259	9.54
2	6	2	50.175	50.159	1.8167	3.39
2	7	0	50.319	50.307	1.8119	2.19

HRTEM image is in a [100] projection, taken close to Scherzer conditions, which means that the black spots in the micrograph can be interpreted as projected columns of metal atoms. The image can be described as built up from two slabs, marked *A* and *B*, of slightly different contrast features. The slabs are parallel to the *c* axis and alternate along the crystal *b* axis. The darker contrast features in slab *A* suggest that most of these spots represent projected W atoms. It should be noted that the dark spots in Fig. 1(*a*) are slightly elongated, probably due to a small crystal tilt. This could be corrected for by applying crystallographic image processing to the HRTEM image.

The processed image in Fig. 1(*b*) shows 64 peaks of density (black spots) in the unit cell, which represent the projected metal atoms in the structure. The supposed symmetry, *Pbcn*, of the crystal is such that there are only ten unique metal atom positions in the unit cell. From the processed image (Fig. 1*b*) the coordinates (y and z) of these atom positions were deduced, of which seven positions were assigned to tungsten and three to neodymium, thus giving a unit cell content of 20 Nd and 44 W atoms. The microanalysis studies gave an Nd:W ratio of ~30:70 at%, which fits well with the proposed model. The W atoms were assigned to the spots with the highest electron-density values. Most of these spots were found in slab *A*. The W atoms were supposed to be located in one plane at $x = 0$, and the neodymium atoms in another plane at $x = \frac{1}{2}$. The length of the *a* axis (~3.8 Å) also suggests that the W atoms are either six- or seven-coordinated in the shape of WO_6 octahedra or pentagonal WO_7 bipyramids, respectively. The polyhedra can be linked through either edge- or corner-sharing in the plane.

A characteristic feature in the HRTEM image (slab *A*), which is even better seen in the processed image, is the star-

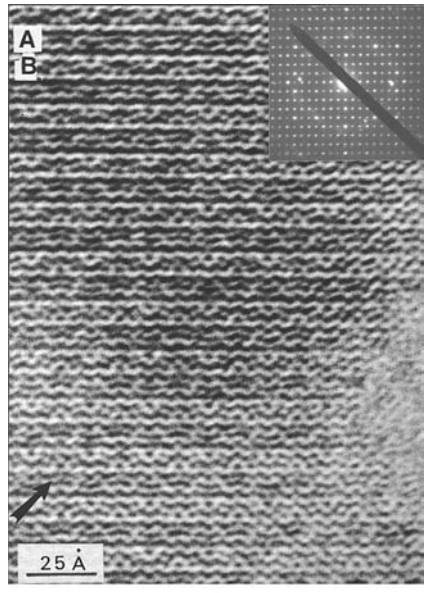

(*a*)

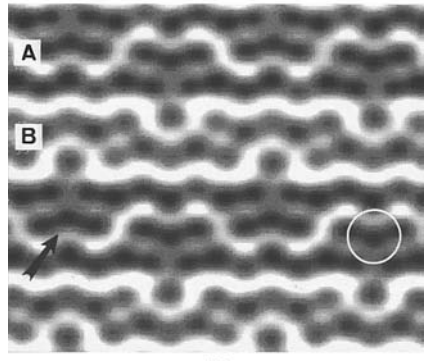

(*b*)

Figure 1
(*a*) HRTEM image of a thin, well ordered crystal fragment projected along [100]. The corresponding ED pattern is inserted. (*b*) The HRTEM image processed with the *CRISP* program (Hovmöller, 1992). The two slabs differing in contrast features and thickness are marked *A* and *B*. The star-shaped units of six black spots, indicating a pentagonal column in the structure, are marked with a white circle in (*b*) and also with arrows in (*a*) and (*b*).

shaped arrangement of six black spots with one spot in the middle surrounded by five spots in a pentagonal arrangement. The star-shaped unit indicates that the structure is built up of pentagonal WO_7 bipyramids with equatorial links to five WO_6 octahedra, thus forming a star-shaped cluster of polyhedra. Along the *a* axis the clusters are stacked on top of each other and linked by corner-sharing, thus forming a pentagonal column, PC (Lundberg, 1971). The HRTEM image and the processed image clearly show that the star-shaped units alternate in a zigzag pattern along the *c* axis. This means that there should be a similar arrangement of PCs in the structure. From these features the O atoms were distributed in the structure model by consideration of available space and W—W distances. Reasonable O atom positions were found by calculation of interatomic W—O and O—O distances. A possible structure model is shown in Fig. 2. The structure can be described as being built up of PCs connected *via* two additional WO_6 octahedra by corner sharing, thus forming a zigzag arrangement of PCs along the *c* axis (slab *A*). All W atoms in slab *A* are located in the same plane. This is in agreement with previously known PC structures such as $W_{12}O_{34}$ (Sundberg, 1978/1979), $K_x(Nb,W)_{17}O_{47}$ (Sundberg & Lundberg, 1987) and $Na_7Nb_{15}W_{13}O_{80}$ (Marinder & Sundberg, 1984).

Fig. 2 also shows that each PC is linked to an ReO_3-type fragment consisting of three WO_6 octahedra, thus forming W_9O_{32} units. These units are stacked on top of each other and linked by corner-sharing, thus forming 'pillars' along the *a* axis. According to the applied symmetry (space group *Pbcn*) the PC slabs form an alternating sequence along the *b* axis, where they are located at $x = 0$ and $x = 0.5$, respectively. Finally, the Nd atoms are located between the tungsten slabs and thus connect them to each other. The composition of the structure model in Fig. 2 is $Nd_{10}W_{22}O_{72}$ ($Z = 2$). Additional O atoms were needed to obtain agreement with the prepared composition, but their locations were not apparent. At this stage an X-ray powder diffraction study using the *EXPO* system (Release 1.01; the integration of programs for Powder Data: Extra + *SirPow* 97 by Altomare *et al.*, 1997) was started, see below.

3.2. X-ray powder diffraction

The *EXPO* (Altomare *et al.*, 1998) system was used to determine a preliminary heavy-atom model of the structure, independent of the electron microscopy study. The centrosymmetric space group *Pbcm* and the formal unit-cell content $Nd_{20}W_{44}O_{162}$ were assumed because of failure to find a reasonable model in *Pbcn* and also because of the absence conditions in the high-angle region discussed above. The option in *EXPO* (Altomare *et al.*, 1998) to exploit the possibility of the Patterson function as prior information for the decomposition of the pattern by the Le Bail technique was successfully applied. The procedure is based on modification and inversion of the Patterson map to obtain new integrated intensities supplied as the starting point for a new extraction process. All heavy-atom positions were approximately determined. By previous information from the electron microscopy study, seven of the ten atom positions were assigned to tungsten and three to neodymium. The *x* coordinates proposed from model building, using the space group *Pbcn*, did not agree, however. The heavy-atom positions were found in two layers, at $x = 0.25$ and $x = 0.75$, respectively. Rietveld refinements with a local version of the program *DBW*3.2S (Wiles *et al.*, 1987) were also used to refine the *x* coordinates of all eightfold metal positions. This made it possible to deduce plausible coordination polyhedra around all W and Nd atoms.

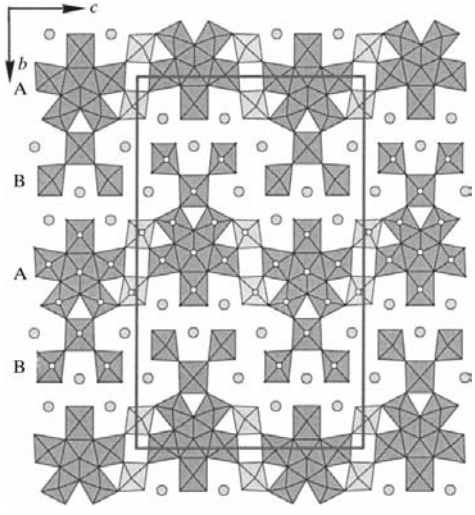

Figure 2
Initial structure model in the [100] projection, deduced from the HRTEM image in Fig. 1 (space group *Pbcn*). The Nd atoms are represented by the large grey circles. The unit cell is outlined. The characteristic W_9O_{32} units, 'pillars', are shaded dark. All structure models are drawn with the program *ATOMS* by Shape Software.

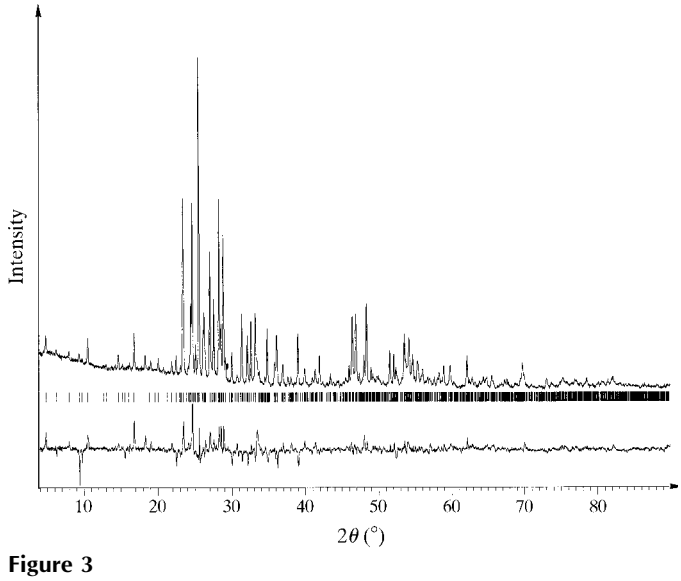

Figure 3
X-ray Rietveld refinement of $Nd_{10}W_{22}O_{81}$. The upper curve illustrates the observed data and the lower curve is the difference between observed and calculated data. The positions of all the allowed Bragg reflections are indicated by the row of vertical tick marks.

The large number of atoms in the unit cell made it necessary to derive oxygen positions purely from geometrical considerations. In the model 156 O atoms could be placed around the W atoms in the unit cell to obtain reasonable W—O and O—O distances. In order to obtain agreement with the prepared composition $Nd_{10}W_{22}O_{81}$, and to obtain a fully oxidized compound, six additional O atoms had to be inserted into the unit cell. One possible eightfold position, O23, was found between two of the Nd atoms, but it can only be occupied to 75%. In the final Rietveld refinement the O atoms were included in fixed positions and only the thermal parameter was refined. The oxygen positions and the refined tungsten and neodymium positions are given in Table 3. The structure-factor *R* value obtained in the final refinement was 0.13. Fig. 3 shows the observed diffractometer data and the difference between the observed and calculated patterns. The crystal structure of $Nd_{10}W_{22}O_{81}$ is shown in Fig. 4 and the metal–oxygen distances are given in Table 4.

A set of simulated images based on the parameters given in Table 3 have been calculated, two of which are shown in Fig. 5. In the defocus region close to Scherzer conditions (*ca* −250 Å) all metal atoms have almost the same dark contrast features, which makes it difficult to distinguish between projected W and Nd atoms in the HRTEM images. However, there is a defocus region close to −100 Å, which yields distinct contrast in the images, so that the characteristic features in the structure are revealed. There is a fairly good agreement between the contrast features in the HRTEM image (Fig. 1*a*) and the calculated image at a defocus value of −120 Å in Fig. 5.

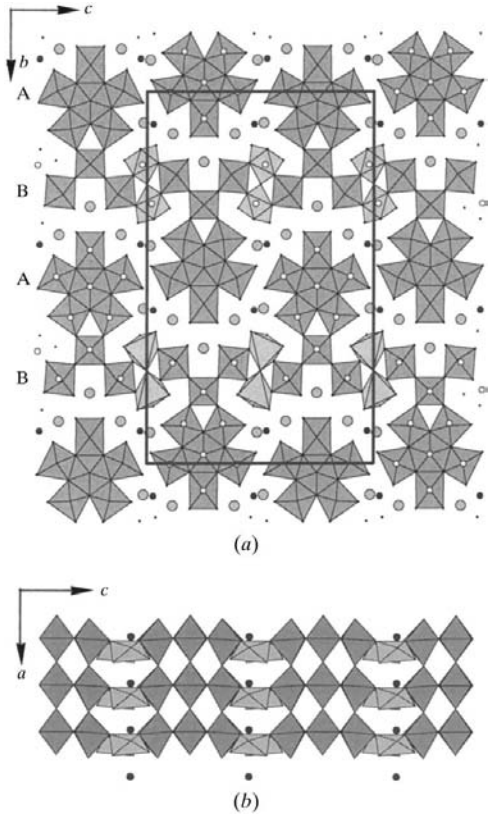

Figure 4
(*a*) Crystal structure of $Nd_{10}W_{22}O_{81}$ (*Pbcm* space group) viewed in the [100] projection. The Nd atoms are represented by large filled circles. The interstitial oxygen (O23), located between two of the Nd atoms, is represented by a small black spot. The characteristic W_9O_{32} units, 'pillars', are shaded dark. The unit cell is outlined. *A* and *B* represent the slabs in the HRTEM image. (*b*) A thin slab (*B*) of the structure viewed in the [010] projection. The interstitial O atoms (black spots) and the W_2O_{11} units (grey) connecting the ReO_3-type fragments are seen.

Table 3
Atomic coordinates of the $Nd_{10}W_{22}O_{81}$ structure.

Atom	Site	*x*	*y*	*z*
Nd1	4(*d*)	0.25	0.1899	3/4
Nd2	8(*e*)	0.7766	0.1139	0.6133
Nd3	8(*e*)	0.7149	0.9157	0.9855
W1	4(*d*)	0.25	0.9755	3/4
W2	8(*e*)	0.1987	0.0015	0.6022
W3	4(*d*)	0.25	0.0732	3/4
W4	8(*e*)	0.2307	0.8928	0.8358
W5	8(*e*)	0.2782	0.1973	0.4794
W6	8(*e*)	0.6705	0.2289	0.6139
W7	4(*d*)	0.25	0.807	3/4
O1	4(*d*)	0.75	0.9755	3/4
O2	4(*d*)	0.25	0.9135	3/4
O3	8(*e*)	0.25	0.0234	0.8115
O4	8(*e*)	0.25	0.9562	0.843
O5	8(*e*)	0.71	0.0018	0.8949
O6	8(*e*)	0.2105	0.0569	0.92
O7	8(*e*)	0.2105	0.9702	0.9817
O8	4(*d*)	0.75	0.0709	3/4
O9	8(*e*)	0.25	0.1195	0.815
O10	8(*e*)	0.7528	0.8994	0.8359
O11	8(*e*)	0.2528	0.843	0.81
O12	8(*e*)	0.22	0.8962	0.9343
O13	8(*e*)	0.17	0.2229	0.63
O14	8(*e*)	0.75	0.268	0.685
O15	8(*e*)	0.6952	0.275	0.56
O16	8(*e*)	0.6952	0.192	0.55
O17	8(*e*)	0.75	0.183	0.68
O18	4(*d*)	0.75	0.8055	3/4
O19	4(*c*)	0.25	1/4	1/2
O20	8(*e*)	0.55	0.345	0.53
O21	8(*e*)	0.23	0.355	0.46
O22	8(*e*)	0.3	0.315	0.6
O23†	8(*e*)	0.22	0.588	0.528

† Partial occupancy ≃ 75%.

3.3. Structure description and discussion

The tungsten framework structure, in Fig. 4(*a*), with the Nd atoms inserted gives a unit-cell content of $Nd_{20}W_{44}O_{156}$ and thus a reduced compound. It does not seem very likely, however, that the obtained product is a reduced neodymium–tungsten oxide, because the compound is synthesized in air from Nd_2O_3 and WO_3. The colour of the product is moreover a faint purple and not the dark blue–black typical of reduced tungsten oxides. An attempt to synthesize the $Nd_{20}W_{44}O_{156}$ compound in an evacuated silica tube resulted in a two-phase mixture of $Nd_2(WO_4)_3$ and a neodymium–tungsten bronze, Nd_xWO_3, of perovskite tungsten bronze type (PTB). In another experiment the initial mixture of 5 Nd_2O_3 + 22WO_3 was heated in an evacuated quartz tube. This synthesis yielded two compounds, our purple phase, identical to the material used in the structure determination above, and a black

Table 4
Average interatomic distances $M-O$ for $Nd_{10}W_{22}O_{81}$.

Coordination No.	$M-O$	Distance (Å)
Seven (WO_7)	W(1)—O	2.11
Six (WO_6)	W(2)—O	2.03
Six (WO_6)	W(3)—O	2.11
Six (WO_6)	W(4)—O	2.04
Six (WO_6)	W(5)—O	2.04
Six (WO_6)	W(6)—O	2.04
Six (WO_6)	W(7)—O	1.93
Eight	Nd(1)—O	2.66
Eight	Nd(2)—O	2.66
Nine	Nd(3)—O	2.47

Nd_xWO_3 tungsten bronze of PTB type. Both additional experiments support the composition $Nd_{10}W_{22}O_{81}$ of our investigated material. The interstitial O atoms seem to be essential for the formation and the stability of the investigated compound. The formula $Nd_{10}W_{22}O_{81}$ ($Z = 2$), can be rewritten as $Nd_5W_{11}O_{39+x}$, with $x = 1.5$ and $Z = 4$, to stress the importance of the interstitial O atoms in the structure. Interstitial O atoms attached only to Ce atoms have been recently reported for $CeTaO_{4.17}$ (Thompson *et al.*, 1999).

The crystal structure in Fig. 4(*a*) resembles that deduced from the HRTEM image in Fig. 2. Both models contain the characteristic structure-building unit, W_9O_{32}. The connections of these units *via* two additional WO_6 octahedra differ, however. In Fig. 4(*a*) the ReO_3-type fragments within slab *B* are located in the same plane and are joined by pairs of tilted WO_6 octahedra (W_2O_{11} groups), thus forming the corrugated layers perpendicular to *b*, as can be seen in Fig. 4(*b*). Owing to the crystal symmetry these layers alternate at $x = 0.25$ and $x = 0.75$ along the *b* axis. The Nd atoms are located in the space between the tungsten layers and form the only link between them. The linkage of the W_9O_{32} units by the pair of tungsten octahedra, the W_2O_{11} group, seems to be new. Several models were tested, and the one presented was chosen as being the most reasonable one.

It is noteworthy that it is impossible to distinguish between the two structure models given in Fig. 2 and Fig. 4(*a*) from HRTEM images projected along the 3.8 Å axis. However, from the ED pattern projected along the *c* axis (3.8 Å) it would have been possible to establish the space group, because reflections with $h + k = 2n + 1$ are systematically present only in *Pbcm*. A large number of ED patterns have been recorded, but none in the [001] orientation have been seen so far, possibly owing to preferred orientation of the crystals. In a few ED patterns weak superstructure reflections have been seen, which indicate a doubling of the 3.8 Å axis. As no indication of a doubled 3.8 Å axis was seen in the X-ray diffraction pattern, this was not taken into consideration in the structure analysis. It seems very likely, however, that the superstructure is caused by some features in the oxygen arrangement.

The structure of $Nd_{10}W_{22}O_{81}$ has only been possible to prepare for the first four lanthanides: La, Ce, Pr and Nd, and not for those with smaller radius. This observation suggests that the size of the *RE* ion is important for the formation of this structure. The crystal structure of $Nd_{10}W_{22}O_{81}$ has some features in common with both $Na_7Nb_{15}W_{13}O_{80}$ (Marinder & Sundberg, 1984) and the tantalates with La and Ce (Kurova & Akesandrov, 1971; Thompson *et al.*, 1999). Fig. 6(*a*) shows that the zigzag arrangement of the PCs in $Na_7Nb_{15}W_{13}O_{80}$ is fairly

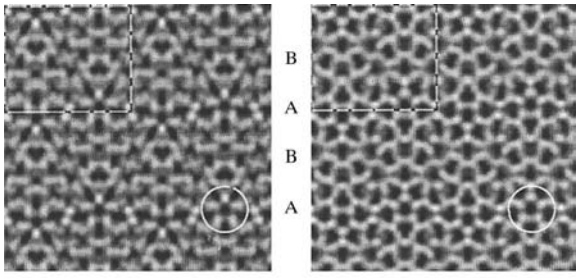

Figure 5
Two simulated images of the structure model $Nd_{10}W_{22}O_{81}$ in the [100] projection. Crystal thickness: ~20 Å; defocus values: (*a*) −120 Å; (*b*) −200 Å. *A* and *B* represent the slabs in the HRTEM image. A pentagonal column is marked with a white circle in both images.

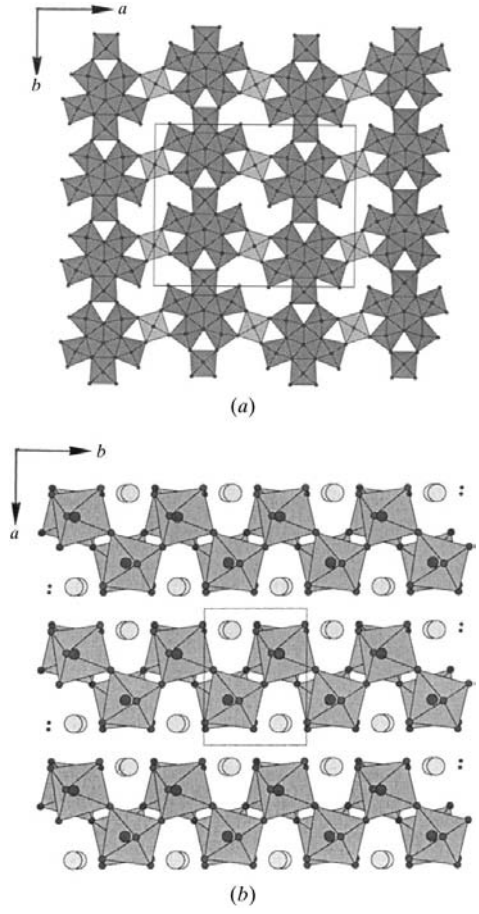

Figure 6
(*a*) The crystal structure of $Na_7Nb_{15}W_{13}O_{80}$ projected along the short 3.8 Å axis. The zigzag arrangement of PCs can be seen along the *a* axis. The Na atoms in the S-shaped tunnels are not shown. The unit cell is outlined. (*b*) The crystal structure of $LaTaO_4$ viewed along the *c* axis. The filled circles represent the La atoms. The unit cell is outlined.

similar to that in $Nd_{10}W_{22}O_{81}$ (Fig. 4*a*) in projection along the 3.8 Å axis. However, the connection of the PCs differs between the two structures. In the $Na_7Nb_{15}W_{13}O_{80}$ structure all PCs are located in the same plane and are connected *via* additional octahedra, thus forming a zigzag arrangement of PCs along the *c* axis. In $Nd_{10}W_{22}O_{81}$ the PCs (slabs *A*) are located in two planes, at $x \simeq 0.25$ and $x \simeq 0.75$ and can thus be considered as isolated. Another characteristic building unit in the structure of $Nd_{10}W_{22}O_{81}$ is the thin slabs consisting of ReO_3-type fragments (slab *B*), joined by pairs of WO_6 octahedra to form the corrugated layers which are approximately two octahedra wide, as can be seen in Fig. 4. It is noteworthy that the rare-earth tantalate structures are built from thin slabs of ReO_3-type, two octahedra wide, as can be seen in the example given in Fig. 6(*b*). In both structures, $Nd_{10}W_{22}O_{81}$ and $LaTaO_4$, the rare-earth atoms form the only link between the tungsten and tantalum slabs, respectively.

In conclusion we note that the combination of X-ray powder diffraction and HRTEM methods has been of great importance in the determination of a plausible structure of $Nd_{10}W_{22}O_{81}$. These results can be used as a good starting point for a more accurate structure determination if single-crystal diffraction data become available in the future.

Financial support from the Swedish Natural Science Research Council is gratefully acknowledged.

References

Altomare, A., Burla, M. C., Carmalli, M., Carrozzini, B., Cascarano, G., Giacovazzo, C., Guagliardi, A., Moliterni, A. G. G., Polidori, G. & Rizzi, R. (1997). *EXPO*, Release 1.01. Universitario di Bari, Italy.

Altomare, A., Foadi, J., Giacovazzo, C., Moliterni, A. G. G., Burla, M. C. & Polidori, G. (1998). *J. Appl. Cryst.* **31**, 74–77.

Hovmöller, S. (1992). *Ultramicroscopy*, **40**, 121–135.

Johansson, K.-E., Palm, T. & Werner, P.-E. (1980). *J. Phys. E*, **13**, 1289–1291.

Kurova, T. A. & Akesandrov, V. B. (1971). *Dokl. Akad. Nauk. SSSR*, **201**, 1095–1098.

Lundberg, M. (1971). *Chem. Commun. University Stockholm* **12**, 1–43.

Marinder, B. O. & Sundberg, M. (1984). *Acta Cryst.* C**40**, 1303–1306.

O'Keefe, M. A., Buseck, P. R. & Iijima, S. (1978). *Nature (London)*, **274**, 322–324.

Shimazaki, T., Yamazaki, T., Terayama, K., Ishiguro, T. & Yoshimura, M. (1999). *J. Alloys Compd*, **285**, 112–118.

Sundberg, M. (1978/1979). *Chem. Scr.* **14**, 161–166.

Sundberg, M. & Lundberg, M. (1987). *Acta Cryst.* B**43**, 429–434.

Thompson, J. G., Rae, A. D., Bliznyuk, N. & Withers, R. L. (1999). *J. Solid State Chem.* **144**, 240–246.

Yoshimura, M., Morikawa, H. & Miyake, M. (1975). *Mater. Res. Bull.* **10**, 1221–1224.

Yoshimura, M., Sata, T. & Nakamura, T. (1973). *J. Chem. Soc. Jpn*, **12**, 2287–2294.

Yoshimura, M., Sibieude, F., Rouanet, A. & Foex, M. (1976). *J. Solid State Chem.* **16**, 219–232.

Werner, P.-E. (1969). *Arkiv Kemi*, **31**, 513–516.

Wiles, D. B., Sakthivel, A. & Young, R. A. (1987). *DBW*3.2s. School of Physics, Georgia Institute of Technology, Atlanta, USA.